LETTER

ACS chemical biology

Isozyme-Specific Fluorescent Inhibitor of Glutathione *S*-Transferase Omega 1

Junghyun Son[†,⊥], Jae-Jung Lee[†,⊥], Jun-Seok Lee[‡], Andreas Schüller[§], and Young-Tae Chang[†,∥,*]

[†]Laboratory of Bioimaging Probe Development, Singapore Bioimaging Consortium, Biomedical Research Council, Agency for Science, Technology and Research, 11 Biopolis Way, 02-02 Helios, Singapore 138667, [‡]Department of Chemistry, New York University, New York, New York 10003, USA, [§]NUS Medicinal Chemistry Programme, Duke-NUS Graduate Medical School, 8 College Road, Singapore 269857, and [∥]Department of Chemistry, National University of Singapore, 1 Science Drive 3, Singapore 117543, [⊥]These authors contributed equally to this work.

ABSTRACT Recently, the glutathione *S*-transferase omega 1 (GSTO1) is suspected to be involved in certain cancers and neurodegenerative diseases. However, profound investigation on the pathological roles of GSTO1 has been hampered by the lack of specific methods to determine or modulate its activity in biological systems containing other isoforms with similar catalytic function. Here, we report a fluorescent compound that is able to inhibit and monitor the activity of GSTO1. We screened 43 fluorescent chemicals and found a compound (**6**) that binds specifically to the active site of GSTO1. We observed that compound **6** inhibits GSTO1 by covalent modification but spares other isoforms in HEK293 cells and demonstrated that compound **6** could report the activity of GSTO1 in NIH/3T3 or HEK293 cells by measuring the fluorescence intensity of the labeled amount of GSTO1 in SDS−PAGE. Compound **6** is a useful tool to study GSTO1, applicable as a specific inhibitor and an activity reporter.

Glutathione *S*-transferases (GSTs) are a family of phase II detoxification enzymes that conjugate reduced glutathione (GSH) to various electrophilic compounds. GSTs are abundant in cells (making up to 10% of cytosolic protein) and consist of at least seven subfamilies such as alpha, kappa, mu, pi, theta, zeta, and omega, and each subclass has several isoforms, respectively (*1*). The diversity of GSTs might explain their various biological roles in detoxification, inflammation, proliferation, apoptosis, etc (*1*). In addition to the physiological functions, GSTs are suspected to be involved in diverse pathological conditions. Many cancers show abnormal profiles of GST isoforms as compared to the ones seen in normal tissues, and the diverse polymorphisms in GSTs are linked to the susceptibility of certain cancers or drug resistances (*2*–*4*). The omega GSTs (GSTO1 and GSTO2) are a newly identified subfamily harboring a cysteine residue in their active site, whereas the other subfamilies have a serine or tyrosine residue (*5*). GSTOs are involved in the detoxification of inorganic arsenical compounds, and mutations or polymorphisms deteriorating their activity are believed to induce arsenicism (*6*). Polymorphisms of GSTOs found in various neoplasms are a potential risk factor, and the overexpression is implicated in the resistance to anticancer therapies (*3, 4*). In addition, certain polymorphisms in GSTO1 appear to be responsible for the susceptibility to or the age at onset of Alzheimer's disease and Parkinson's disease (*6*). However, their pathological roles are still controversial since the functional study of each isoform is limited because of the diversity, complexity, and functional similarity of GSTs (*1*). Thus, isoform-specific modulators or reporters are truly required (*7*).

In previous studies we have employed the technique of proteome profiling using chemically reactive fluorescent compounds as a tool for functional genomics (*8*). Generally, chemically reactive fluorescent dyes have been used for *in vitro* labeling of specific functional groups (amine and thiol) in proteins, and this reaction renders the dyes to be nonreactive toward other proteins. However, we observed that diverse derivatives of fluorescent compounds themselves recognize different macromolecules due to subtle alterations in the structure. In order to correlate the proteome staining profiles with the structural differences, we screened reactive fluorescent dyes together with their various derivatives by SDS−PAGE.

Forty-three commercial compounds were applied to the live NIH/3T3 cells, and the labeling profile was analyzed in gel (Supplementary Figure S1). While most probes showed a similar profile within the same fluorescent scaffold, six fluorescein derivatives exhibited considerably different pat-

*Corresponding author, chmcyt@nus.edu.sg.

Received for review October 15, 2009 and accepted March 5, 2010.

Published online March 5, 2010

10.1021/cb100007s

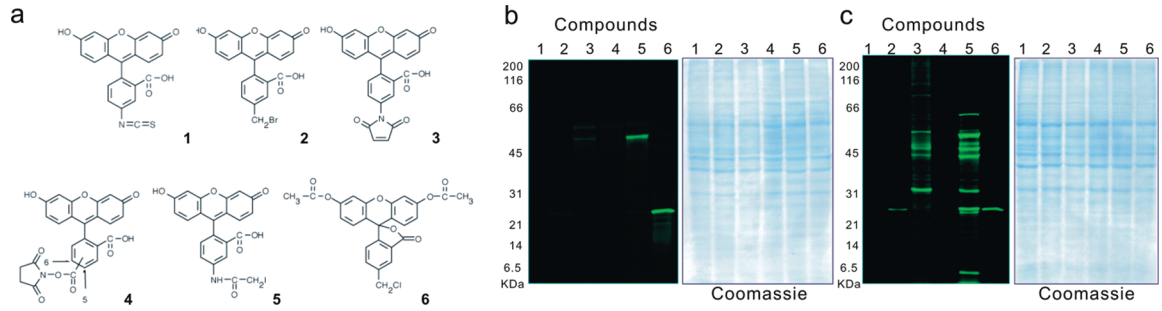

Figure 1. Proteome staining profiles of fluorescent compounds. a) Structure of six fluorescein derivatives among 43 fluorescent compounds screened. Protein labeling by six fluorescein derivatives analyzed by SDS—PAGE with staining under live conditions (NIH/3T3 cells) (b) or when treated to total lysates of NIH/3T3 (c). Fluorescent gel image was taken from the FITC channel (Ex 488 and Em 520 nm) and the coomassie staining of the respective gel is shown.

terns. Two of them have amine-reactive groups (isothiocyanate **1** and succinimide **4**), and the other four have thiol-reactive groups (benzyl halides **2** and **6**, maleimide **3**, and iodoacetyl **5**) (Figure 1, panel a). Each probe labeled proteins of different size with different efficiency (Figure 1, panel b), affected by the chemical reactivity, proximity to reactive residues, affinity to targets, etc. For compounds **2** and **6**, cell permeability would be another critical factor affecting their labeling efficiency. While compound **6** may pass more freely through cell membranes, compound **2** may be less membrane-permeable (*9*). Furthermore, compound **6** might be transformed into the chlorobenzyl analogue of compound **2** by intracellular esterase (*9*). To address how cell permeability affects the labeling profile, we treated those six fluorescein derivatives to cell lysates instead of live cells (Figure 1, panel c). Indeed, compound **2** showed better labeling efficiency without the membrane barrier, and the labeling pattern of compound **3** was quite different from the staining under live cell conditions. Among the six probes, compounds **2** and **6** labeled a single band (Figure 1), and further analysis by 2D-PAGE also revealed a single stained spot (Supplementary Figure S2).

In order to develop a specific probe for a single protein, we identified the labeled protein and modification site by 2D-HPLC combined with mass spectrometry (MS) (Supplementary Figure S3). The sole fluorescent peak was purified from compound **6**-treated NIH/3T3 lysate by size exclusion chromatography (SEC) (Supplementary Figure S4, panels a and b) and was digested and analyzed through reverse-phase (RP)-HPLC-MALDI TOFMS with MASCOT proteome database search (http://www.matrixscience.com) (*10*).

The MS/MS analysis identified the single fluorescent peak from the RP-peptide separation as mouse GSTO1, and the binding site was Cys32 of the peptide 31-FCPFAQR-37 (Figure 2, panels a and b). The *y* and *b* ion fragments of Cys32 bound to compound **6** were detected in a MS/MS ion search (Figure 2, panel b), and a strong immonium ion (*m*/*z* 345) was detected in MS/MS spectra of compound **2**-tagged peptide (Figure 2, panel a), a bromobenzyl analogue of compound **6** (Figure 2, panel b).

Then, we assessed the specificity of compound **6** by EGFP fusion proteins of the respective GST isoforms. We generated EGFP fusion constructs of seven human GSTs (alpha1, kappa1, mu1, pi1, theta1, zeta1, and omega1) (Supplementary Table S2). Those recombinant GSTs were expressed in HEK293 cells individually, and cells were incubated with 500 nM of compound **6** for 1 h. Among the recombinant GSTs, only exogenous GSTO1 exhibited a fluorescent band that was confirmed as the recombinant protein (GSTO1-EGFP) by Western blotting (Figure 2, panel c).

Recently, the commercial fluorescent probe HaloTag diAcFAM Ligand (Promega) was reported to show a similar proteome staining profile (*11*). The authors pointed out the structural similarity between the HaloTag diAcFAM Ligand and compound **6** (personal communication). Therefore, we suspected that GSTO1 could be an endogenous target of this compound and observed that HaloTag diAcFAM Ligand indeed stained the exogenous GSTO1 (Supplementary Figure S5, panels a and b). Although both compounds bind to a common protein, the diAcFAM Ligand was less efficient in staining GSTO1 than compound **6**; 0.2 μM compound **6** produced a comparable fluorescent intensity as acquired by 10 μM HaloTag diAcFAM Ligand (Supplementary Figure S5, panel c).

Compound **6** has the potential to serve as a catalytic inhibitor since it binds to the active site covalently. To address whether compound **6** inhibits only GSTO1 and not other isoforms, we measured the enzyme activity of individual GST isoforms after treatment with compound **6** in live cells. After transfecting the plasmids encoding EGFP-fusion protein of the GST kappa1, pi1, or omega1, we incubated the HEK 293 cells with compound **6** for 1 h. Then, the exog-

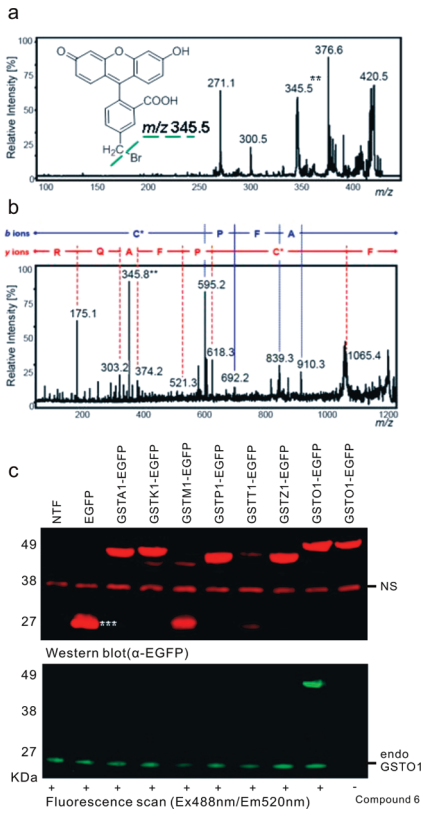

Figure 2. Identification of target protein and binding sites. a) MS/MS spectrum of compound 2 to detect a specific immonium ion, *m/z* 345, after cleavage of bromine by laser-induced decomposition. b) MS/MS ion search of the fractionated peptide fluorescent peak. * The series of *y* and *b* ions including compound 6-tagged Cys detected. ** The specific immonium ion (*m/z* 345) was observed. c) Fluorescence scanning of the SDS−PAGE and Western blotting of EGFP to confirm the expression of EGFP-GSTs in HEK293 cells. "NS" represents nonspecific band recognized by an α-GFP antibody and is shown as the quantification control. * The EGFP expressed from pEGFP-N1 without fusion of GST; endoGSTO1 is the endogenous GSTO1 stained by compound 6.**

enous GSTs were purified by immunoprecipitation from total lysate using an EGFP antibody and subjected to an enzyme assay. The inhibition was specific to GSTO1 in a concentration-dependent manner with a half-maximal inhibitory concentration (IC_{50}) of 51 nM (Figure 3, panels a and b). The inhibition was irreversible and lasted up to 180 min after treatment of compound **6** in EGFP-GSTO1 transfected HEK293 cells (Figure 3, panel c).

The intrinsic fluorescence of compound **6** inspired us to develop it as a fluorescent probe to detect functionally active GSTO1. We treated Ebselen to live NIH/3T3 or HEK293 cells and then stained the cells with compound **6**. Ebselen is a GST inhibitor affecting the active cysteine residue (*12*). A gradual reduction in the fluorescence intensity for GSTO1 was observed in the presence of Ebselen in both cell lines in a concentration-dependent manner (Figure 3, panel d). We could monitor the residual activity of GSTO1 with compound **6** by measuring the fluorescence intensity of the corresponding band on gel and calculated the IC_{50} of Ebselen in NIH/3T3 (IC_{50} = 13 μM) and HEK293 cells (IC_{50} = 12 μM). These results suggest that compound **6** is suitable for the activity monitoring of GSTO1.

To elucidate a potential mode of interaction between compound **6** and GSTO1, we docked the hydrolyzed species of compound **6** (equivalent to the chlorobenzyl analogue of compound **2**) into the crystal structure of human GSTO1 (Protein Data Bank code: 1eem) (*13*). Redocking experiments with glutathione were performed with GOLD version 4.1 (The Cambridge Crystallographic Data Centre) (*14*) to verify the suitability of the target for docking. The crystal structure pose of GSH in the G-site subpocket was well reproduced with an average rmsd of 0.54 ± 0.06 Å for non-hydrogen atom coordinates and a favorable GoldScore of 67.70 ± 0.68 (mean value ± SD of 10 repetitions). Covalent docking of the chlorobenzyl analogue of

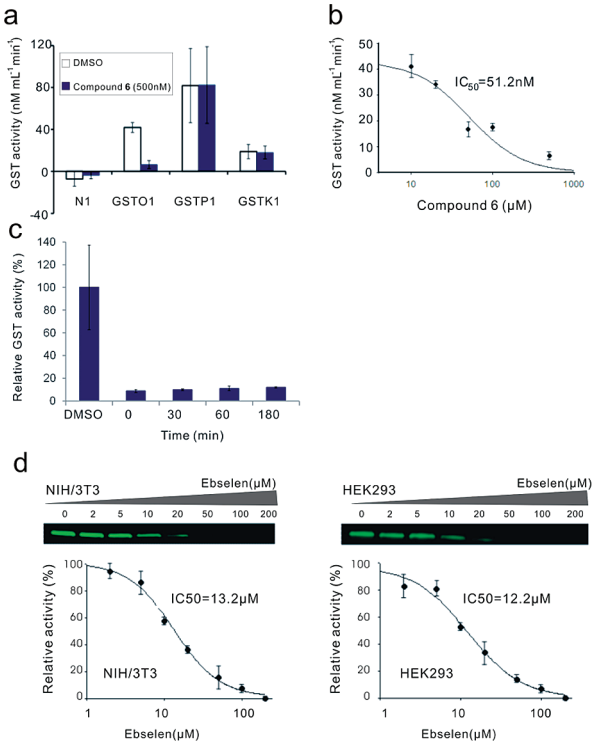

Figure 3. Compound 6 is a GSTO1-specific inhibitor and fluorescent reporter. Exogenously expressed fusion proteins were immunoprecipitated, and the activity of respective isoform was measured. a) Activity of GSTs after treatment with compound 6 at a concentration of 500 nM for 1 h. IC_{50} of compound 6 on GSTO1 was calculated as 51.2 nM. c) A time-course study showing persistence of GSTO1 inhibition by compound 6. GSTO1-EGFP was transfected into HEK293 cells, and compound 6 was treated. After 1 h of incubation with compound 6, cells were washed, and a group of cells were harvested (T0). Other groups of cells were incubated in fresh medium and harvested at 30, 60, or 180 min after washing. Enzyme activity of the immunoprecipitated GSTs is shown as the relative % activity comparing to the activity from the DMSO-treated sample. d) Visualization of the active GSTO1 in gel using compound 6 after pretreatment of Ebselen in NIH/3T3 and HEK293 cells.

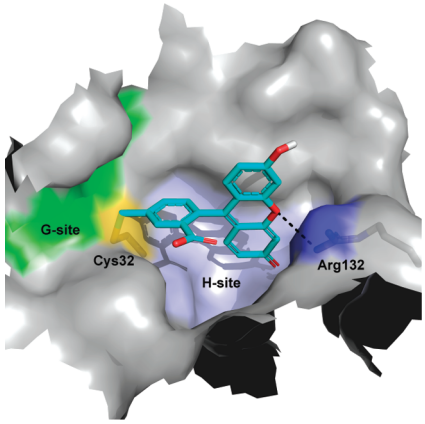

Figure 4. Molecular docking of the intracellular transform of compound 6 to GSTO1 (PDB code: 1eem) by GOLD v4.1. The compound covalently bound to the thiol sulfur of the active site Cys32. Docking predicted binding to the H-site (light blue) with largely hydrophobic interactions (GoldScore: 31.40 ± 0.06). A weak hydrogen bond to Arg132 seems possible (dashed line). Green, G-site subpocket; cyan, carbon atom; red, oxygen atom; dark blue, nitrogen atom; yellow, sulfur atom; and white, hydrogen atom. Figure generated with PyMOL v1.1r1 (DeLano Scientific).

compound **2** into the binding site of GSTO1 in contrast suggested binding to the H-site subpocket of the GST binding site (Figure 4). The average GoldScore of 31.40 ± 0.06 indicated favorable binding with a moderate binding affinity. The docking algorithm converged well on a single cluster of binding poses with an average pairwise rmsd of 0.19 ± 0.08 Å. The H-site of hGSTO1 forms a wide and deep, largely hydrophobic pocket adjacent to the glutathione binding site (G-site) (*13*). Besides the covalent bond, the predicted binding mode was dominated by hydrophobic interactions with GST.

In summary, we report a new GSTO1-specific inhibitor. Compound **6** inhibits specifically GSTO1 while sparing other isoforms in live cells. Considering the diverse biological functions of GSTs, a specific inhibitor blocking a single isoform would have a versatile usage in biological study. Without a specific inhibitor, the functional study of a gene should depend on laborious methods such as a systematic gene knockout or RNAi. Therefore, a small molecule-based inhibitor would be a convenient and cost-effective way to study an enzyme. Moreover, compound **6** is fluorescent by itself. It allows visualization of the active GSTO1 in the total proteome, especially when the active site of the target enzyme is intact. We prepared several serial deletion constructs of GSTO1 as EGFP fusion proteins. When compound **6** was applied to the cells expressing those deletion mutants, compound **6**-stained band was not observed from any of the mutants, although the catalytic Cys32 was preserved in them (data not shown). Thus, not only the active site but also the structural intactness is crucial for binding of compound **6**. Hence, the functional status of GSTO1 in live cells can be read out by compound **6**. Previously, chemical probes to monitor the activity of certain enzymes, such as the ABPP (activity-based protein profiling) probes, have been developed. ABPP monitors catalytically active enzymes rather than their total amounts and indeed provides a better understanding for the functional status of the enzymes in the given biological system (*15*). For example, Cravatt's group developed the ABPP probes for metabolic enzymes including GSTO1. Sulfonate ester ABPP probe enabled profiling of the functional status of GSTO1 in the proteomes of cancer samples (*16*). Mostly, the ABPP probes require profound rational designs to introduce the bulky reporters (fluorophore, biotin, or both), which limit the high-throughput development and the *in vivo* applicability (*15*). Screening chemically reactive fluorescence libraries can be an alternative to the challenging rational design, as was demonstrated here by the identification of compound **6**, an activity reporter of GSTO1. Additionally, we suggest a careful choice of the fluorophores in biological applications. Fluorescein derivatives are widely used for protein labeling linked to antibodies, nucleotides, or ligands to trace the labeled proteins. However, unintended tagging by reactive fluorophores might occur. The HaloTag diAcFAM Ligand would be an example of unintended labeling of a nontargeted cellular protein, the GSTO1 (Supplementary Figure S5).

METHODS

Cell Culture. Mouse fibroblast (NIH/3T3) and human embryonic kidney cells (HEK293) were grown in Dulbecco's Modified Eagle Medium (DMEM, GIBCO) supplemented with 10% (v/v) fetal bovine serum and penicillin/streptomycin (100 μg mL^{-1}) in a humidified atmosphere at 37 °C with 5% (v/v) CO_2.

Screening. The fluorescein derivatives, purchased from Invitrogen (Supplementary Table S1) were treated to live cells at 500 nM in normal medium. After 1 h of incubation at 37 °C, cells were washed with PBS and lysed in CellLytic M buffer (Sigma). Total protein extracts were boiled with Laemmli sample buffer (Bio-Rad) including 5% (v/v) 2-mercaptoethanol (Bio-Rad) and analyzed in the 10.4−14% (w/v) polyacrylamide gel containing 0.1% (w/v) SDS (Bio-Rad) at a constant voltage 120 V. Gels were immediately scanned on a Typhoon9400 scanner (Amersham Bioscience).

2D-HPLC. Cell lysate was separated by fluorescence-based 2D-HPLC combined with SEC and RPC. SEC was performed by Phenomenex BioSep S2000 column (300 mm × 7.8 mm i.d.) with a mobile phase of 100 mM sodium phosphate (pH 7.0) with an isocratic flow rate of 1 mL min^{-1} on Shimadzu ultra fast liquid chromatography (UFLC). The fluorescent peak (Ex 488 and Em 520 nm) in SEC was reconstituted in 6 M urea (1% v/v acetic acid) after complete evaporation of the mobile phase by a refrigerated CentriVap concentrator (LABCONCO). C18 reversed phase chromatography was performed by an Agilent mRP column (50 mm × 4.6 mm, ID) with a mobile phase: (A) 0.1% (v/v) trifluoroacetic acid (TFA) and (B) acetonitrile with 0.1% (v/v) TFA with nine-steps programmed gradient (Supplementary Table S3).

HPLC-MALDI-ToF MS/MS Analysis. The fluorescent fraction of the C18 RPC for peptide separation, performed by a Phenomenex Luna C18 (150 mm × 4.6 mm i.d., 5 μm) column with mobile phase: (A) 0.1% (v/v) TFA and (B) acetonitrile with 0.1% (v/v) TFA with six-steps programmed gradient (Supplementary Table S4), was evaporated and reconstituted in 0.1% (v/v) TFA solution, and 0.5 μL of the sample was applied onto a 600 μm AnchorChip (Bruker Daltonics). When the droplet size reached the size of the Anchor, 2 μL of matrix solution (0.3 g L^{-1} of α-cyano-4-hydroxy cinnamic acid in ethanol/acetone 2:1) was applied onto the droplet. We used a 2,5-dihydroxybenzoic acid (DHB) matrix to mix equal volumes of sample and matrix (5 g L^{-1} DHB, 0.1% v/v TFA in water containing 30% v/v acetonitrile) and applied 1 μL onto a 600 μm AnchorChip to archive a crystal rim preparation. Bruker Daltonics Ultraflex III with

SmartBeam and MASCOT search engine were used for peptide mass fingerprinting and MS/MS ion search of the digested fluorescent peak to determine the molecular target and binding site (Figure 2, panels a and b).

Fusion Protein and Western Blotting. Total RNA prepared from human normal dermal fibroblasts was used for cDNA synthesis, and ORF of seven isoforms of GST (alpha1(GSTA1), kappa1(GSTK1), mu1(GSTM1), pi1(GSTP1), theta1(GSTT1), omega1(GSTO1), and zeta1(GSTZ1)) were PCR-amplified (Supplementary Table S2) and inserted into the EcoR1/BamH1 sites of the pEGFP-N1 (Clontech). Identity of the acquired clones was confirmed by nucleotide sequencing. Approximately 5×10^5 cells well^{-1} of HEK293 were seeded into a 6-well plate and 1 μg of DNA was transfected by using Lipofectamine 2000 (Invitrogen). Total protein extract from the transfected cells was subjected to Western blotting. Antibodies used are mouse monoclonal anti-GFP antibody (Santa Cruz, sc-9996) and goat antimouse IgG (H+L)-Cy5 (Zymed, 81-6516).

Immunoprecipitation and GST Assay. HEK293 cells were transfected with plasmids encoding EGFP-GSTs, and the pEGFP-N1 was transfected as a negative control encoding only EGFP. Transfected cells were incubated at the indicated concentrations of compound **6** for 1 h, and total protein was extracted. Two micrograms of EGFP antibody were added to 500 μg of lysate and incubated by slow agitation at 4 °C. On the following day, 50 μL of Protein-G agarose (Roche) was mixed with the protein extract and incubated by slow agitation at 4 °C for 6 h. Agarose beads were precipitated by centrifugation, resuspended in 50 μL of PBS, and subjected to an enzyme assay or Western blotting. GST activity was determined by a GST assay kit (Sigma). This assay measures the increase in absorbance at 340 nm due to the conjugation of GSH to 1-chloro-2,4-dinitrobenzene (CDNB) (*17*).

Molecular Docking. The structure of hGSTO1 in complex with GSH was downloaded from the Protein Data Bank (code: 1eem) and processed with the Molecular Operating System (MOE) version 2008.1001 (Chemical Computing Group) as follows: (i) water molecules and sulfate ions were removed; (ii) hydrogens were added,and their positions were optimized with Protonate 3D at pH 7; (iii) the complex was energy minimized (force field AMBER99 with Generalized Born solvation model (*18*), final gradient 0.05 kcal mol^{-1} Å^{-1}, heavy atoms tethered) and (iv) saved for docking after removal of glutathione. Molecular docking was performed with GOLD version 4.1 (The Cambridge Crystallographic Data Centre) as follows: (i) binding site definition: solvent accessible atoms in a 15-Å radius sphere centered on carbon CD of Pro33; (ii) scoring function: GoldScore with automatic settings, 200% search efficiency, no early termination; (iii) covalent docking: enabled, ligands attached to the thiol sulfur of Cys32. Docking simulations were repeated 10 times each with 10 initializations of the docking algorithm.

Acknowledgment: This work was supported by intramural funding from A*STAR Biomedical Research Council and National University of Singapore Young Investigator Award (R-143-000-353-123). J.-S.L. thanks the POSCO TJ Park Foundation (TJ Park Bessemer Science Fellowship) for generous support.

Supporting Information Available: This material is available free of charge *via* the Internet at http://pubs.acs.org.

REFERENCES

1. Dourado, D. F., Fernandes, P. A., and Ramos, M. J. (2008) Mammalian cytosolic glutathione transferases, *Curr. Protein Pept. Sci. 9*, 325–337.
2. Davies, S. M., Bhatia, S., Ross, J. A., Kiffmeyer, W. R., Gaynon, P. S., Radloff, G. A., Robison, L. L., and Perentesis, J. P. (2002) Glutathione *S*-transferase genotypes, genetic susceptibility, and outcome of therapy in childhood acute lymphoblastic leukemia, *Blood 100*, 67–71.
3. Marahatta, S. B., Punyarit, P., Bhudisawasdi, V., Paupairoj, A., Wongkham, S., and Petmitr, S. (2006) Polymorphism of glutathione *S*-transferase omega gene and risk of cancer, *Cancer Lett. 236*, 276–281.
4. Townsend, D. M., and Tew, K. D. (2003) The role of glutathione-*S*-transferase in anti-cancer drug resistance, *Oncogene 22*, 7369–7375.
5. Whitbread, A. K., Masoumi, A., Tetlow, N., Schmuck, E., Coggan, M., and Board, P. G. (2005) Characterization of the omega class of glutathione transferases, *Methods Enzymol. 401*, 78–99.
6. Schmuck, E. M., Board, P. G., Whitbread, A. K., Tetlow, N., Cavanaugh, J. A., Blackburn, A. C., and Masoumi, A. (2005) Characterization of the monomethylarsonate reductase and dehydroascorbate reductase activities of omega class glutathione transferase variants: implications for arsenic metabolism and the age-at-onset of Alzheimer's and Parkinson's diseases, *Pharmacogenet. Genomics 15*, 493–501.
7. Mahajan, S., and Atkins, W. M. (2005) The chemistry and biology of inhibitors and pro-drugs targeted to glutathione *S*-transferases, *Cell. Mol. Life Sci. 62*, 1221–1233.
8. Lee, J. S., Kim, Y. K., Vendrell, M., and Chang, Y. T. (2009) Diversity-oriented fluorescence library approach for the discovery of sensors and probes, *Mol. Biosyst. 5*, 411–421.
9. Haugland, R. P. (2005) *The Handbook; A Guide to Fluorescent Probes and Labeling Technologies*, 10th ed., Invitrogen, Carlsbad, CA.
10. Karas, M., and Hillenkamp, F. (1988) Laser desorption ionization of proteins with molecular masses exceeding 10,000 Da, *Anal. Chem. 60*, 2299–2301.
11. Gautier, A., Juillerat, A., Heinis, C., Correa, I. R., Jr., Kindermann, M., Beaufils, F., and Johnsson, K. (2008) An engineered protein tag for multiprotein labeling in living cells, *Chem. Biol. 15*, 128–136.
12. Nikawa, T., Schuch, G., Wagner, G., and Sies, H. (1994) Interaction of ebselen with glutathione *S*-transferase and papain *in vitro*, *Biochem. Pharmacol. 47*, 1007–1012.
13. Board, P. G., Coggan, M., Chelvanayagam, G., Easteal, S., Jermiin, L. S., Schulte, G. K., Danley, D. E., Hoth, L. R., Griffor, M. C., Kamath, A. V., Rosner, M. H., Chrunyk, B. A., Perregaux, D. E., Gabel, C. A., Geoghegan, K. F., and Pandit, J. (2000) Identification, characterization, and crystal structure of the omega class glutathione transferases, *J. Biol. Chem. 275*, 24798–24806.
14. Jones, G., Willett, P., Glen, R. C., Leach, A. R., and Taylor, R. (1997) Development and validation of a genetic algorithm for flexible docking, *J. Mol. Biol. 267*, 727–748.
15. Speers, A. E., and Cravatt, B. F. (2004) Chemical strategies for activity-based proteomics, *ChemBioChem 5*, 41–47.
16. Jessani, N., Humphrey, M., McDonald, W. H., Niessen, S., Masuda, K., Gangadharan, B., Yates, J. R., 3rd, Mueller, B. M., and Cravatt, B. F. (2004) Carcinoma and stromal enzyme activity profiles associated with breast tumor growth *in vivo*, *Proc. Natl. Acad. Sci. U.S.A. 101*, 13756–13761.
17. Habig, W. H., Pabst, M. J., Fleischner, G., Gatmaitan, Z., Arias, I. M., and Jakoby, W. B. (1974) The identity of glutathione *S*-transferase B with ligandin, a major binding protein of liver, *Proc. Natl. Acad. Sci. U.S.A. 71*, 3879–3882.
18. Labute, P. (2008) The generalized Born/volume integral implicit solvent model: estimation of the free energy of hydration using London dispersion instead of atomic surface area, *J. Comput. Chem. 29*, 1693–1698.